XL CILAMCE
IBERO-LATIN AMERICAN CONGRESS ON COMPUTATIONAL METHODS IN ENGINEERING
NOVEMBER 11-14, 2019
Praiamar Natal Hotel & Convention Natal, RN-BRAZIL

BEARING CAPACITY ANALYSIS OF PILES THROUGH FINITE ELEMENT: CASE STUDY HERCÍLIO LUZ BRIDGE, SANTA CATARINA, BRAZIL

Gabriel D. Andrade
Gracieli Dienstmann
gabrieldibe1@gmail.com
g.dienstmann@gmail.com
Department of Civil Engineering, Federal University of Santa Catarina,
Street Eng. Agronômico Andrei Cristian Ferreira, s/n - Trindade, 88040-900, Florianópolis - SC, Brazil

Abstract. Soil engineering has progressed through the gathering of building experiences and the development of theoretical knowledge, allowing the creation of estimating techniques for the ultimate resistance of a foundation element. This ultimate resistance is known as bearing capacity and represents the maximum load acting on the foundation element. On what concerns pile foundations, it is noted a significant difficulty to establish the theory that completely describes the bearing capacity of piles. Thus, different methods aiming to estimate the bearing capacity are currently used, for instance, the semiempirical methods (Aoki-Velloso, Décourt-Quaresma, and others) and the finite element method. In the present paper the bearing capacity of the foundation massif of Hercílio Luz Bridge, located in Santa Catarina, Brazil, will be evaluated through a finite element model of an isolated pile. The pile was modeled using the software Abaqus v. 6.13, considering an axisymmetric model and linear elastic behavior. The latter was submitted to an axial compression load until failure. The soil surrounding the pile was modeled considering the Mohr-Coulomb elastoplastic model. To determine parameters as cohesion, friction angle, and Young Modulus for the soil, literature correlations with Standard Penetration Test (SPT) were used. Numerical results were compared to semiempirical values and a loading test. It was noted that the outcome of the finite element method provided lower bearing capacity than the semiempirical methods and the results of the loading test.

Keywords: Bearing capacity of piles; Semiempirical methods; Finite elements method; Bidirectional static load test.

1 Introduction

The development of foundations knowledge has enabled the creation of techniques for determining the resistance of a pile foundation element. When the soil strength of the pile element is evaluated the term bearing capacity is applied. Bearing capacity in conjunction with the prediction of displacement is an essential component of foundation geotechnical design and ensures the safety of the superstructure. For deep foundations, the bearing capacity consists of two components: the normal strength of the tip and the lateral frictional resistance of the shaft.

The complexity of the study for deep foundations lies in the determination of an appropriate physical and mathematical model that expresses with good approximation the failure. The difficulty in defining the bearing capacity theoretically has led to a different approach of the technical community. Semiempirical methods came up as a proposal to establish the correlation between in situ tests, such as SPT or CPT, and bearing capacity. In Brazil, the use of the Standard Penetration Test (SPT) is commonly employed and for this reason, established Brazilian methods usually have correlations with this test.

At present, another approach to the determination of bearing capacity consists of the use of the Finite Element Method (FEM). The principle of this method rests upon the discretization in small elements and establishment of a system of equations that respect boundary conditions. The FEM requires the knowledge of modeling and more robust computational tools. The result obtained is more detailed, but the professional who uses the software must pay attention to the simplifications made for the required soil behavior, as well soil concrete interactions.

Apart from these methods that seek to determine the bearing capacity during foundation design, the load tests, known as direct methods, aim to verify the built foundation element through load application. The result of these tests is commonly a load versus displacement curve. With this curve, it is possible to verify if what was determined by some of the previously mentioned methods matches the reality.

In the present paper, the Finite Element Method (FEM) is used to determine the bearing capacity of one pile belonging to the foundations of the Hercílio Luz Bridge anchorage massif. The values obtained from modeling are compared with semiempirical methods as well as with results of the bidirectional static load test.

2 Study case

This paper focuses on the study case of the anchorage massif foundation of Hercílio Luz Bridge. The rehabilitation of the structure, located in the municipality of Florianópolis (SC), has begun in 2016 and by 2018 has achieved the stage of foundation's construction.

This chapter presents the characteristics of the construction, soil profile investigation, and bidirectional static load test data.

2.1 New anchorage massif characteristics

The massif consists of a concrete block with approximately 3.300 m³ whose geometry is shown in Fig. 1 (a). The massif, located in the continental ending of the bridge, transfer load from the eye-bars to ground through its weight and a group of pile foundation.

According to the technical report PHL.TD.005.NT011 [1] the eye-bars transfer to the massif (ultimate limit stage according to NBR 6118 [2]) 66.706 kN, in the horizontal axis, and 33.109 kN, in the vertical axis, resulting in 74.471 kN. Besides, the massif weight is approximately equal to 82.500 kN.

The project defines the demolishment and the rebuilt of the original massif (built in the 1920s) due to its old age and the difficulty to determine the integrity of foundation elements, a group of eucalyptus piles. The concrete bored piles substituted the old wood piles. However, the original wood piles had not been removed before the bored pile's construction. Furthermore, the pile cap of the original structure has been maintained. Fig. 1 (b) shows a 3D model of the new massif.

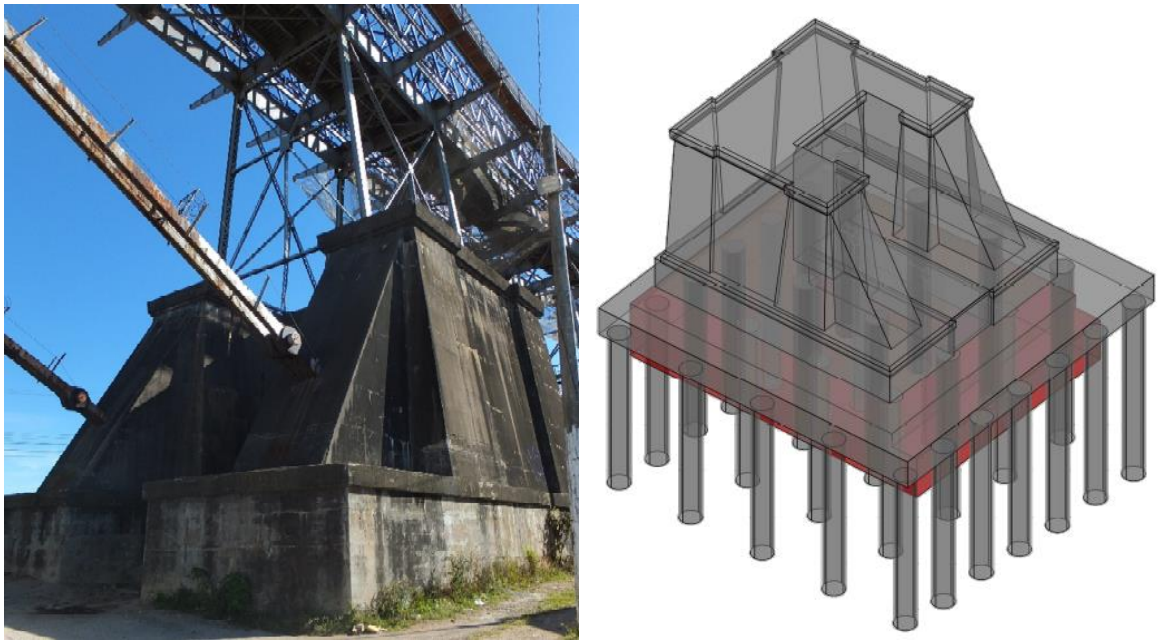

Figure.1 (a) Original continental Anchorage massif - Figure.1 (b) new anchorage massif 3D model

The new foundation consists of 29 concrete bored piles, each pile with 1.5 m diameter and 15 m length. Fig. 2 presents part of the foundation design. From the same image, it is also noted the group of bored piles exceeding the original massif's dimensions (in red). The new pile cap is a concrete block with sides of 24.30 x 24.70 and 2.00 m height, resulting in a volume of 1.200 m³.

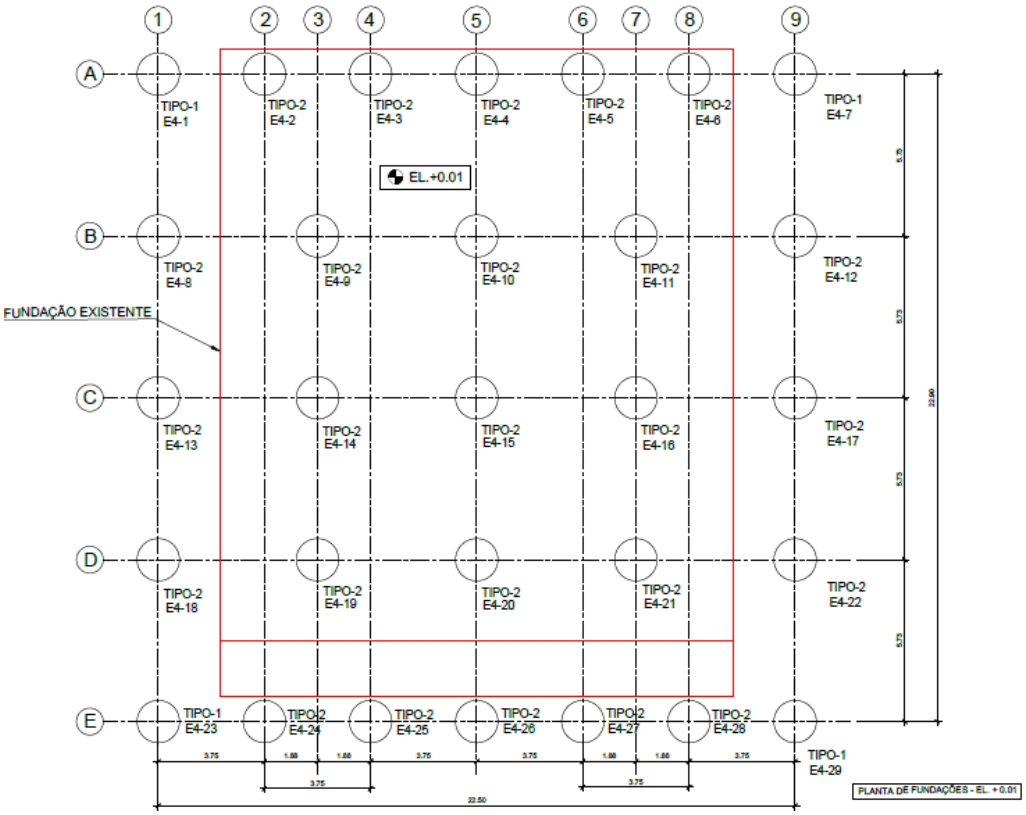

Figure 2. Foundation design – piles location

2.2 Soil profile

In April 2016 EMPA company, responsible for the rehabilitation of Hercílio Luz bridge, contracted Sotepa company to conduct a soil investigation, from which this paper has obtained soil data. According to Fig. 3, Sotepa drilled 4 boreholes nearby the continental anchorage massif. The outcome of the soil investigation is presented as a soil profile for each hole in Figs. 4 to 7.

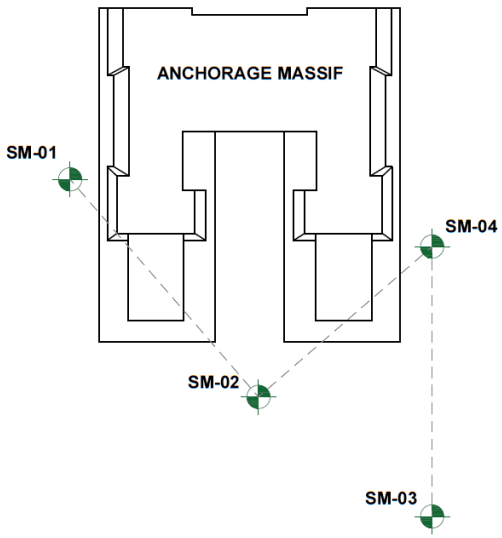

Figure 3. Approximate location of the 4 boreholes

Soil investigation profile defined as SM-01 is located on the south face of the massif, near the middle portion of the block length. The soil investigated is composed of 3 layers with thicknesses around 5,00 m: grayish coarse sand, yellowish silty sand, and orange sandy silt. The groundwater table is verified at a 15.30 m depth.

Resistance in SM-01 region increases with depth: the first layer, grayish coarse sand, has an average N_{SPT} of 8; the second layer, yellowish silty sand, has an average N_{SPT} of 14; and the third layer, orange sandy silt, has an average N_{SPT} of 22.

The soil profile defined by SM-02 sounding is located at the midpoint of the massif width, between SM-01 and SM-04 soundings. In this soil profile, there is also the presence of 3 layers: yellowish coarse sand, yellowish silty coarse sand, and orange sandy silt. Layer thicknesses are more distinct, unlike SM-01. The first layer has a thickness of 2.50 m, the second of 4.30 m and the third of 7.00 m. The altered rock occurs at 14.80 m depth while the groundwater table occurs at 3.70 m.

The evolution of resistance with depth for SM-02 sounding is shown in Fig. 5, where a practically constant resistance up to 6.00 m is observed. From this point on, the N_{SPT} value presents two abrupt variations at depths 7 m and 10 m, where N_{SPT} practically doubles. Thus, the evolution of resistance is not so smooth, especially in the sandy silt layer. The first layer, yellowish coarse sand, has an average N_{SPT} of 6, the second layer, yellowish silty coarse sand, has an average N_{SPT} of 10, and the third layer, orange sandy silt, has an average N_{SPT} of 30.

SM-03 sounding is located on the north side of the massif and is closer to the sea. The results, shown in Fig. 6, indicate that the soil is composed of 3 layers: brownish sand, grayish coarse sand, and orange sandy silt. The thicknesses of the last two layers are approximate, the second with 7.30 m and the third with 6.1 m. The thickness of the first layer is only 3.20 m. Groundwater table occurs at 3.50 m.

The change of N_{SPT} is SM-03 region is smooth in the first layer and most of the second. The more expressive variation of this value occurs at the interface between the grayish coarse sand and the sandy silt. The first layer, brownish medium sand, has an average N_{SPT} of 7, the second layer, grayish coarse sand, has an average N_{SPT} of 17, and the third layer, orange sandy silt, has an average N_{SPT} of 32.

SM-04 sounding is also located on the north face of the massif. The soil profile, Fig. 7, indicates a greater number of layers than has been verified on the others profiles, a total of 4, whose composition is: brownish medium sand, grayish coarse sand, orange medium sand with gravel, and orange sandy silt.

What concerns layer thickness, the first and the last layer have approximately 5.5 m whereas the two intermediate layers have around 2.0 m. The groundwater table occurs at 0.20 m.

Regarding the values of N_{SPT} for SM-04 region, this profile presents a different variation from the trend of the others. There is an increase of resistance at the beginning of the intermediate layers and also an abrupt reduction at the end of them. It is noted that when reaching the orange sandy silt layer, a large gain in soil resistance is observed. The first layer, brownish medium sand, has average N_{SPT} of 7; the second layer, grayish coarse sand, has average N_{SPT} of 18; the third layer, orange medium sand, has average N_{SPT} of 12; and the fourth layer, orange sandy silt, has an average N_{SPT} of 36.

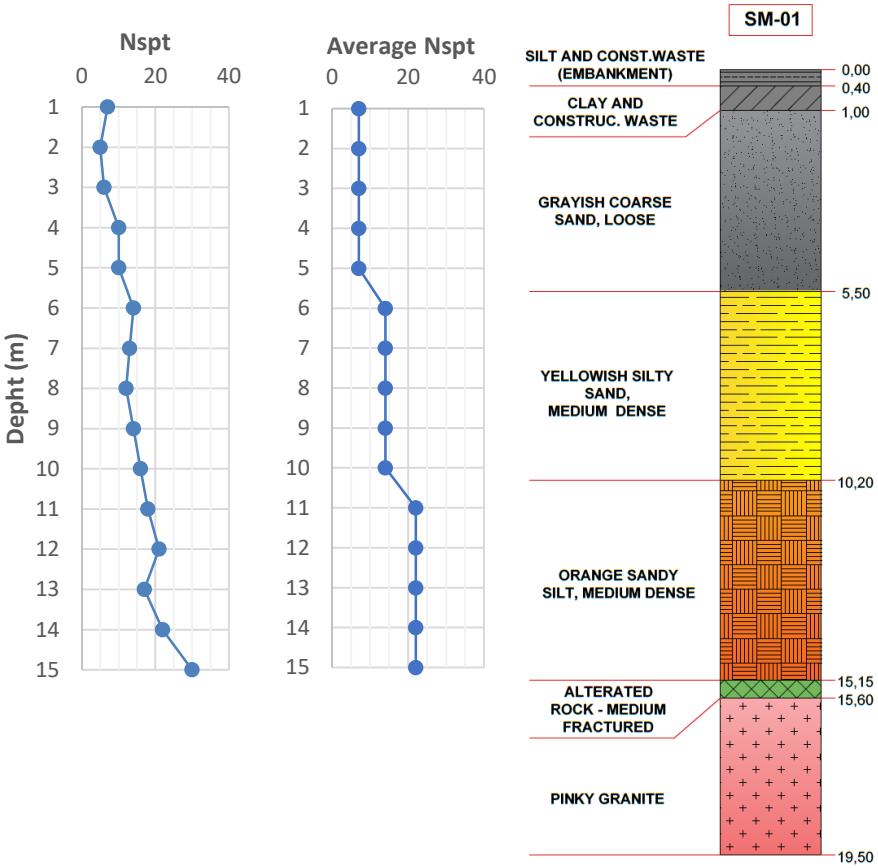

Figure 4. Outcome of the borehole SM-01

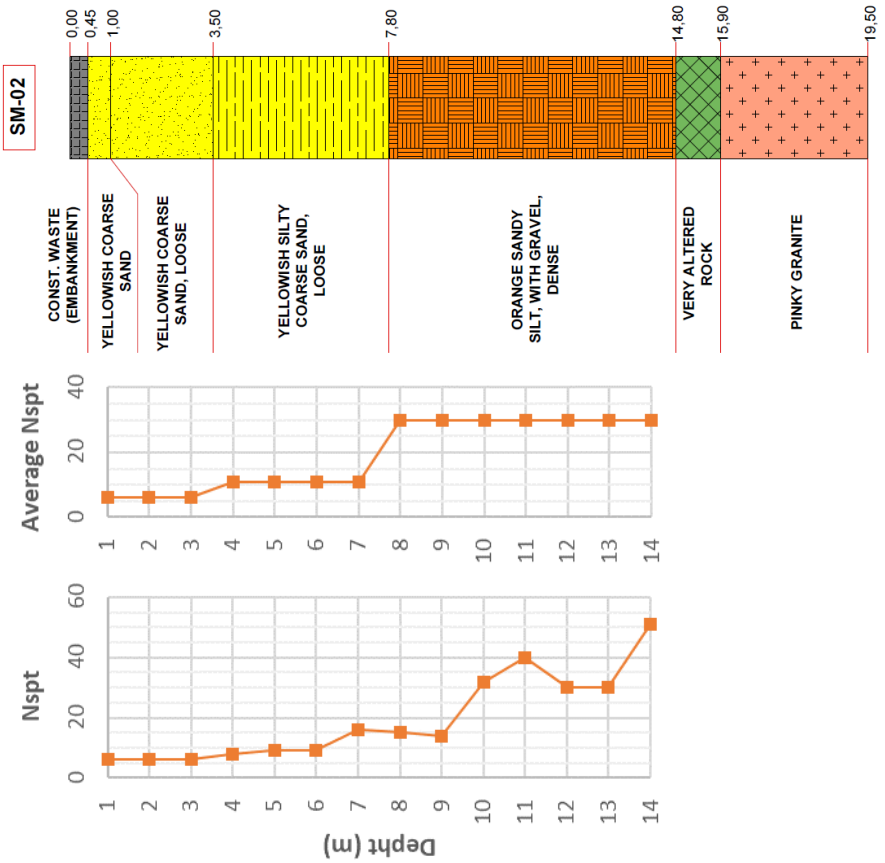

Figure 5. Outcome of the borehole SM-02

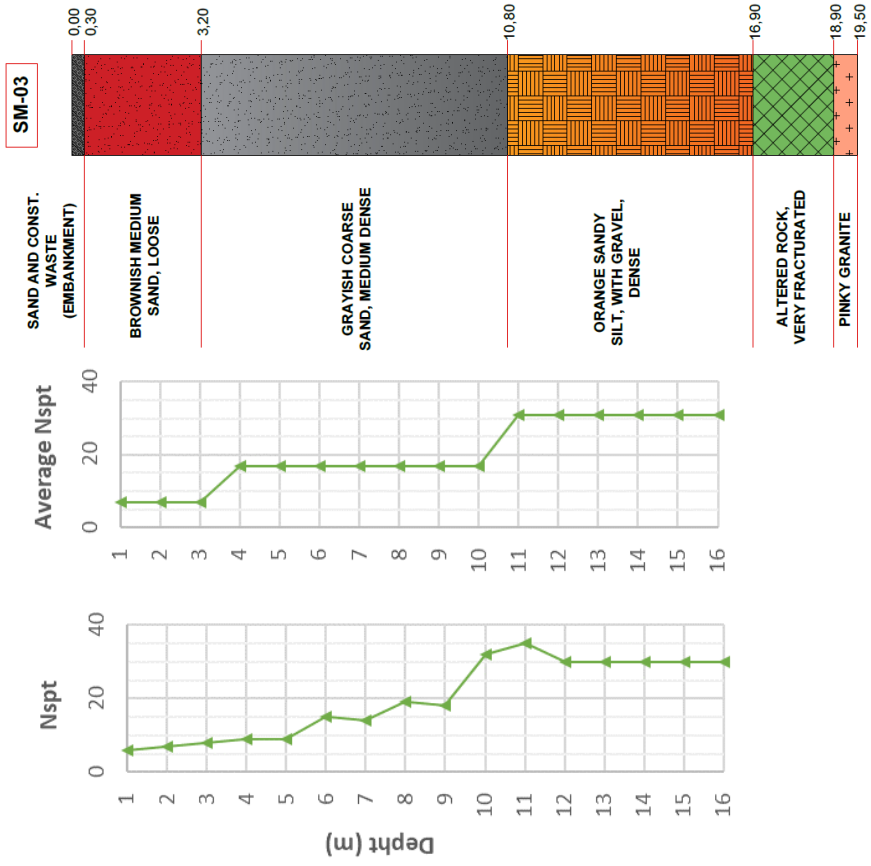

Figure 6. Outcome of the borehole SM-03

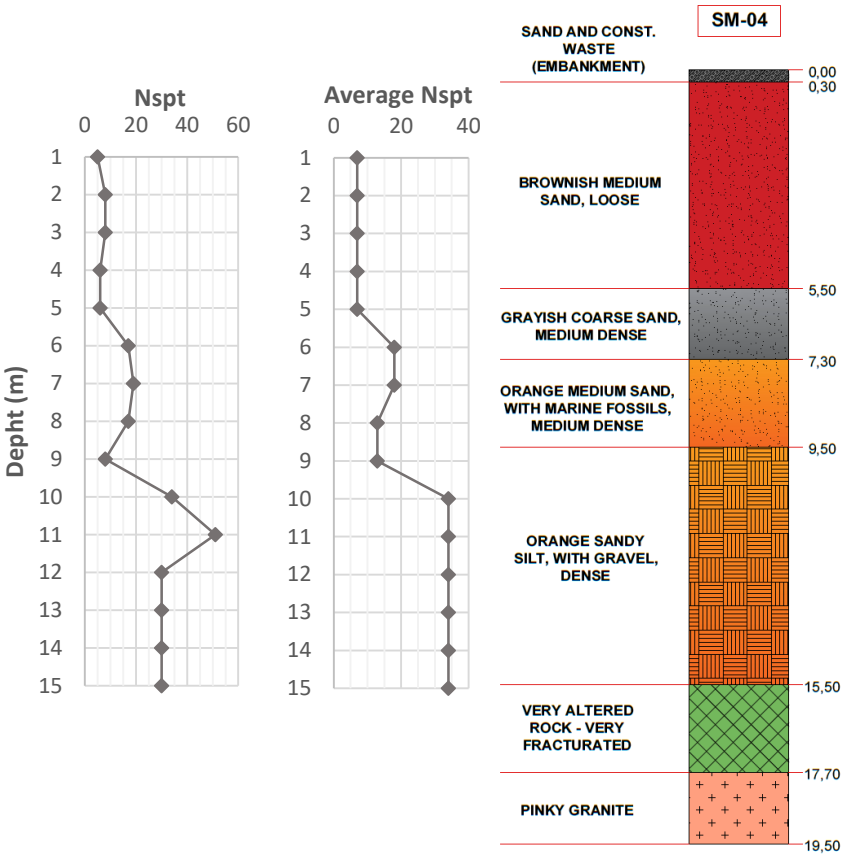

Figure 7. Outcome of the borehole SM-04

2.3 Bidirectional static load test

According to technical report PHL.TD.005.NT016 [3] a bidirectional static load test was performed. Arcos company has carried out this loading test, in which hydrodynamic expansive cells, a total of three, were positioned at 12.17 m depth, close to the pile toe. Only pile E4-23 was tested, since NBR 6122:2010 [4] requires that 1% of the number of piles to be tested. From Fig. 2 and 3 it is noticed that soil profile according SM-01 is the nearest to the tested pile, 6.8 m approximately.

The positioning of expansive cells took place on August 23rd, 2018, and loading test was carried out on October 2nd. A period, corresponding to 41 days, was necessary to allow cure and strength gain of concrete.

E4-23 has been loaded until 7,656.00 kN (pile tip plus shaft strength) without geotechnical rupture verification. The mentioned report presents 13,418.5 kN as designed bearing capacity and 3,530 kN as maximum working load. Fig. 8 showd the curve: axial load versus displacement. Table 1 presents more details of the bidirectional static load test.

The data from Table 1 and Fig. 8 indicate that the displacements are more pronounced in the shaft than those obtained in the pile toe (tip) for a same stress. A maximum displacement around 5 mm is characterized in both positions measuring shaft strength (pile head and above expansive cells – upper cells), while 1.27 mm maximum displacement is defined to the same loading at the tip.

Table 1. Bidirectional static load test data

Loading test	Segment	Measure-ment	D (cm)	Length (m)	Loading method	Max. Loading (kN)	Max. Displac. (mm)	Residual Displac. (mm)
PCE-03	Above exp. Cells (shaft)	Pile head	150	15,00	Fast	3.828,0	5,31	2,27
PCE-03	Above exp. Cells (shaft)	Above exp. cells	150	15,00	Fast	3.828,0	5,52	2,47
PCE-03	Under exp. Cells (tip)	Lower exp. cells	150	15,00	Fast	3.828,0	1,27	0,41

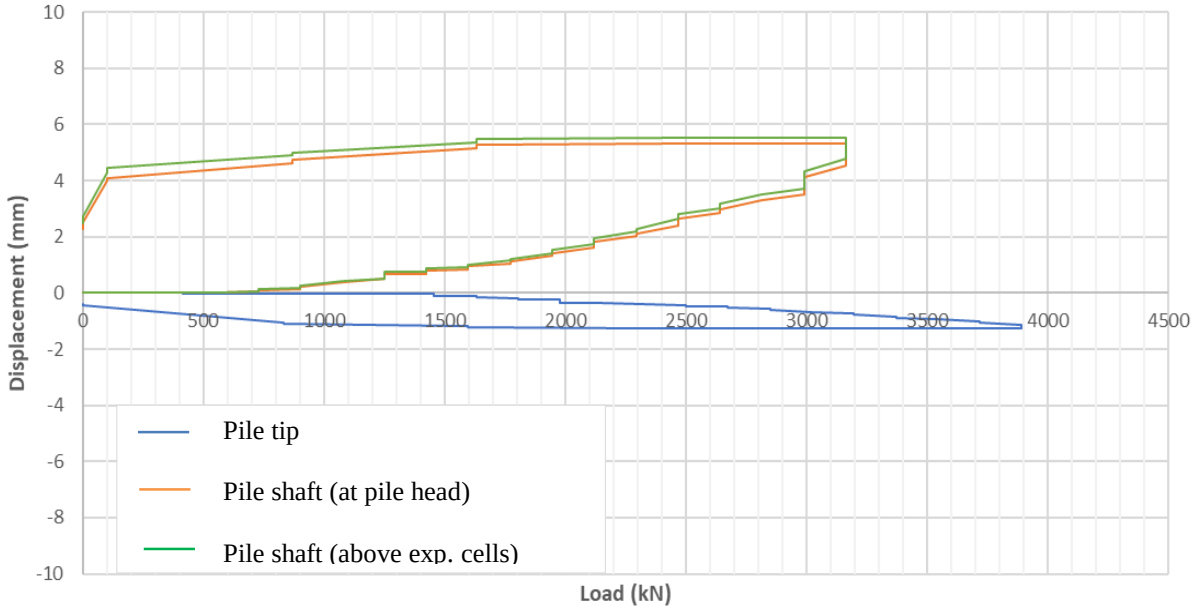

Figure 8. Load x displacement curve (measurement at pile head and above expansive cells)

3 Bearing capacity analysis

In the present chapter the results of bearing capacity obtained through the FEM modeling for Hercílio Luz bridge massif foundation, the interpretation of bidirectional static load test results and the comparison with semiempirical methods are presented and discussed.

3.1 Bidirectional static load test results (PCE-03)

From the analysis of Fig. 8, it is clear that the magnitude of displacements between pile tip and the two measurements related to the shaft (pile head and above expansive cells) are different. This characteristic makes the procedure suggested by Silva [5] for construction of the equivalent curve difficult since it is not possible to establish a correlation for the same displacements. Furthermore, the bidirectional static load test has not reached geotechnical failure, which is defined as an infinite progressive displacement at a constant load, corroborating the need for curve extrapolation.

Extrapolation has been elaborated separately for the shaft and the pile tip. For this procedure it was not necessary to consider the unloading data, thus we limited the used data until the third step of stage

22, the last load increment.

Van der Veen [6] method was applied for the pile tip extrapolation curve. According to Eq. (1) the maximum tip resistance (R_{tip} maximum) for best curve fit is equal to 5,500 kN. Fig. 9 illustrates the extrapolation. On the other hand, Eq. (2), representing the pile shaft, indicates maximum shaft resistance (R_{shaft} maximum) equal to 3,320 kN for the best curve fit. Fig. 10 illustrates the extrapolation.

$$R_{tip} = 5{,}500\ (1 - e^{0{,}88082\ z}) \tag{1}$$

$$R_{shaft} = 3{,}320(1 \quad - e^{-0{,}4327\ z}) \tag{2}$$

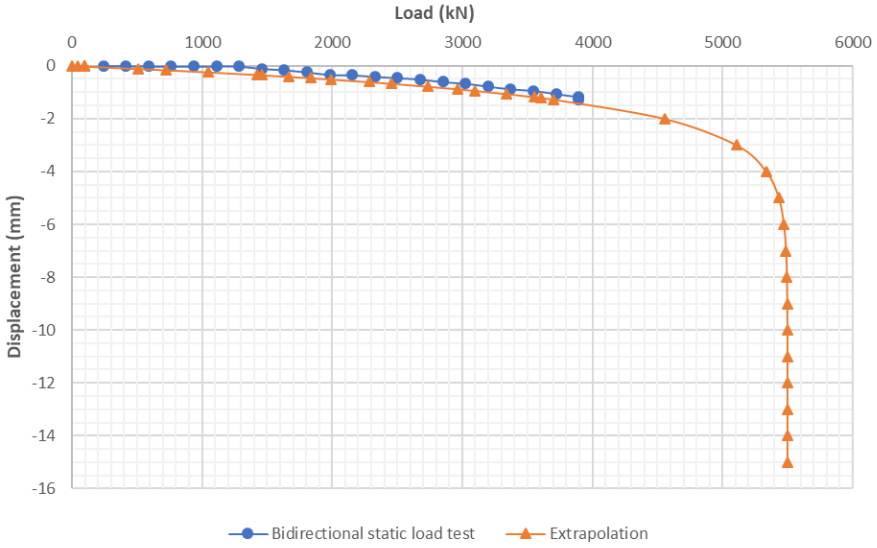

Figure 9. Comparison between load test and extrapolation (pile tip)

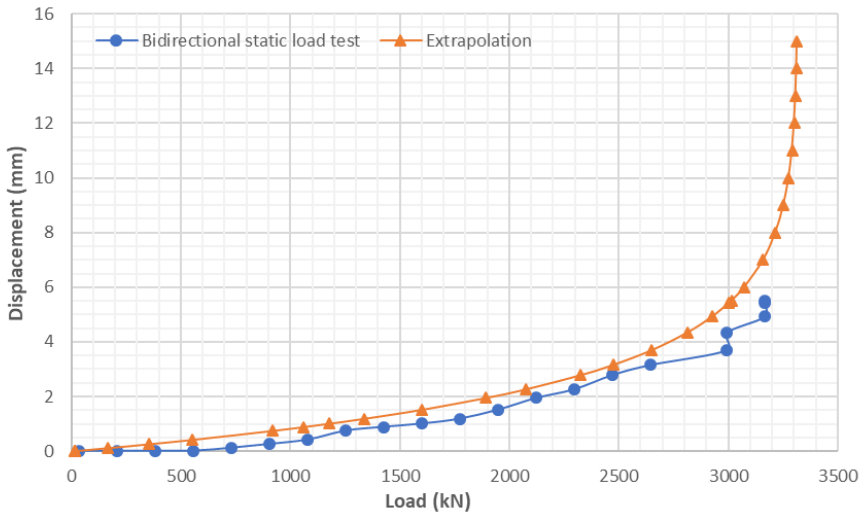

Figure 10. Comparison between load test data and extrapolation (shaft)

The extrapolation equations allow employing the procedure created by Silva [5] and Falconi and Maset [7] to create the equivalent curve. Thus, initially, we set displacement values and then calculate loading values through the equations previously defined.

Regarding the method of Falconi and Maset [7], it was found that the calculation of elastic pile shortening is insignificant when compared to displacement. The order of the values obtained is 10^{-7} and 10^{-6} m. This verification is explained by the high rigidity of the pile, mainly related to the large diameter of 1.5 m and the high concrete modulus, 34 GPa according to NBR 6118: 2014 [2]. Therefore, the difference between the equivalent curves according to Silva [5] and Falconi and Maset [7] is not noticeable.

Fig. 11 presents the equivalent curve and the interpretation of NBR 6122 [4] for the geotechnical failure load. The criterion defines failure through an elastic shortening added to a diameter-related displacement. It is noted, given the negligible value of pile shortening, that the correlation with diameter governs the rupture criterion. Thus, the failure displacement is 50 mm (1500mm/30), forming a horizontal line that intersects the equivalent curve and indicates 8,820 kN as bearing capacity.

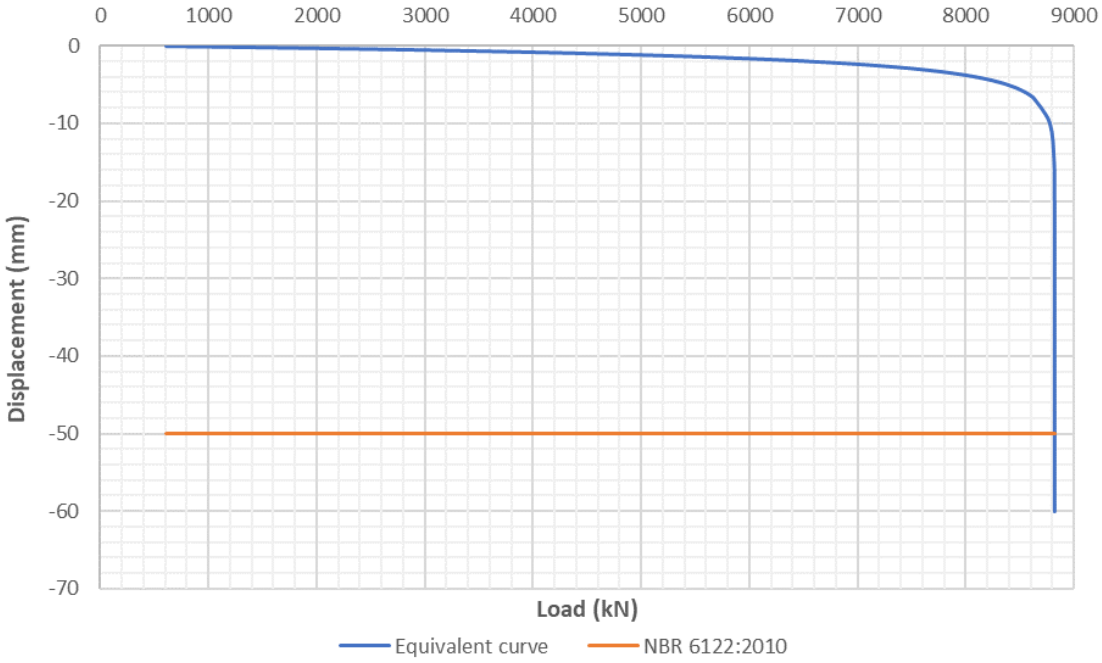

Figure 11. Equivalent curve and rupture criterion according to NBR 6122:2010

3.2 Evaluation of bearing capacity through finite element method (FEM)

In the present paper, the software Abaqus CAE version 6.13 has been employed for modeling the bored pile of the case study and soil layers determined by soil investigation. The model employed was axisymmetric, which consists of a 2D approximation of a 3D problem. The pile geometry and the surrounding soil, when modeled in a FEM, allow stress, strain, and displacement to be characterized. The later can be directly used to predict pile displacements which are generally not addressed in semiempirical methods. Although, attention must be paid to the limitations of the adopted constitutive criteria. For this paper, pile elements are considered linear elastic and the surrounding soil was modeled considering an elastoplastic material with a Mohr-Coulomb type of failure.

A total of 13,668 axisymmetric elements of a quadrilateral 4-axis bi-linear node with reduced integration (CAX4R) are used in the analysis. Fig. 12 shows the general model and mesh discretization. Boundary conditions are defined as: horizontal displacement restriction on the lateral and base boundaries and restriction of vertical displacements on the base.

Soil parameters were evaluated for each investigation region. In this case empirical correlations based on N_{SPT} measurements or typical values of soil or rock according to technical literature were considered.

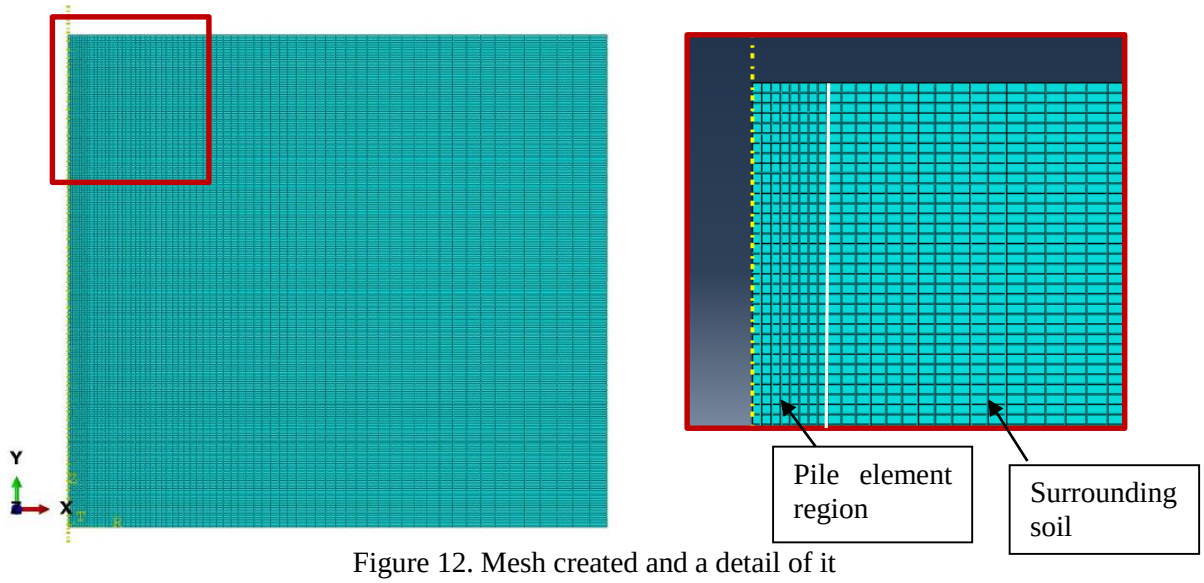

Figure 12. Mesh created and a detail of it

Correlations presented in Cintra et al. [8] has been used to determine the parameter's value from N_{SPT} of each soil layer: Elastic Modulus (E) and Poisson's ratio (ν) according to Teixeira and Godoy (1996), Specific weight according to Godoy (1972) and Friction angle (ϕ) according to Godoy (1983).

In the case of soil layers of depth less than 1.0 m, typical values were adopted for these materials. These initial layers are basically composed of silt, clay, and sand. The cohesion value for sandy soil layers was set at 1 KPa to avoid numerical instability.

For rock formations, the parameters were obtained from Vallejo [9] and for modeling simplification, only elastic properties of the rocks were considered. For the altered rock, it was decided to apply a reduction of approximately 50% in the value of the modulus (E) and specific weight in relation to the value of Pink Granite.

Tables containing the adopted parameters to each site investigation are presented in the next sections.

3.3 Modeling results for SM-01

The parameters adopted for this investigation region are presented in Table 2. Results of the numeric evaluation are presented in Figs. 13 and 14, concerning shear and axial stress. The trends presented in these figures represent the general behavior of all regions modeled (SM-01 to SM-04). Generally, the formation of equipotential surfaces propagates from the pile tip to the soil and rock layers. Also, it was noted the presence of an element near the external face of the pile that has a higher value than the nearby elements.

Table 2. Soil parameters for SM-01 model

Soil	Average N_{SPT}	E (MPa)	ν	Specifc weight (kN/m³)	ϕ (°)	C (Pa)
Silt	-	2.65	0.3	15	19	$2.50x10^4$
Clay	-	2.65	0.2	15	19	$2.50x10^4$
Grayish coarse sand	7	18.9	0.2	16	30.8	$1.0x10^3$
Yellowish silty sand	14	29.4	0.3	17	33.6	$1.0x10^3$
Orange Sandy silt	22	49.5	0.4	18	36.8	$1.0x10^3$
Altered rock	-	$2.0x10^4$	0.2	20	-	-
Pinky granite	-	$4.7 x10^4$	0.2	26	-	-
Concrete 45MPa	-	$3.40 x10^4$	0.2	25	-	-

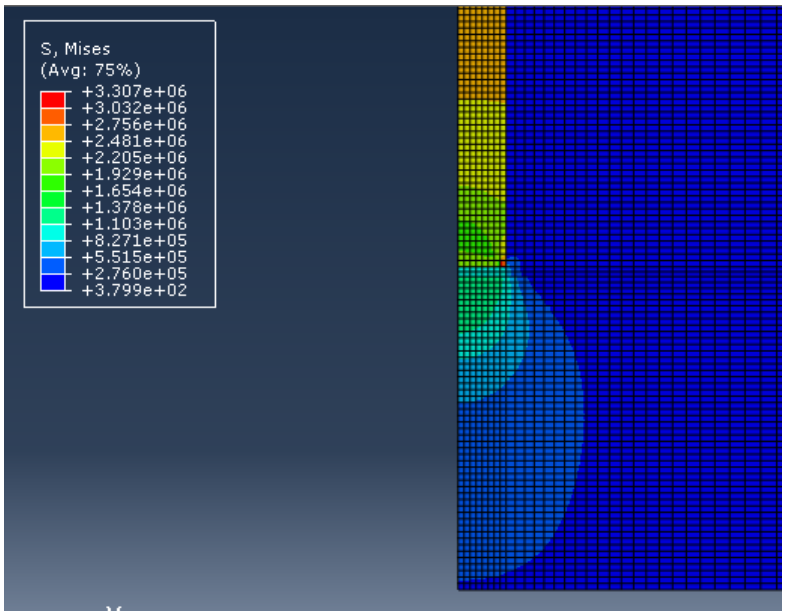

Figure 13. Shear stress (Pa) for SM-01 model

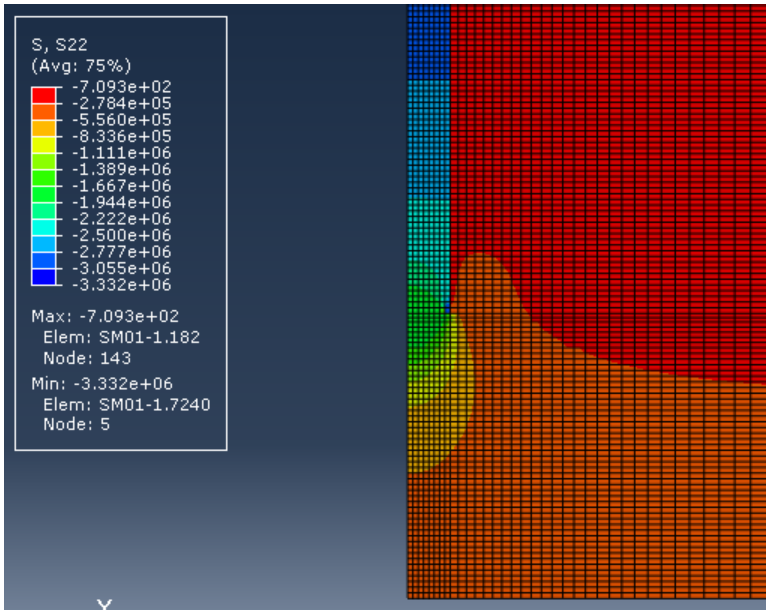

Figure 14. Normal stress (Pa) for SM-01 model

For shear stress, for region SM-01 the maximum value corresponds to 3.31 MPa while the minimum value is 0.38 KPa. The maximum value of normal stress is 3.33 MPa and the minimum is 0.71 KPa. Maximum values are usually found at the pile head while the minimum values are found in distant regions.

Displacements are more pronounced in the upper part of the foundation element and tend to decrease with increasing horizontal distance, as shown in Fig. 15. This figure also well represents the general behavior of all regions modeled (SM-01 to SM-04). The maximum displacement is 4.20 mm in the same direction of the loading.

For the creation of a load versus displacement curve, the node on the pile surface near to the symmetry axis (left edge) was adopted. With stress and displacement values for this node, it was possible to elaborate the displacement load curve according to Fig. 16. In this case the maximum stress value is 5,853.76 kN with a displacement of 4.19 mm.

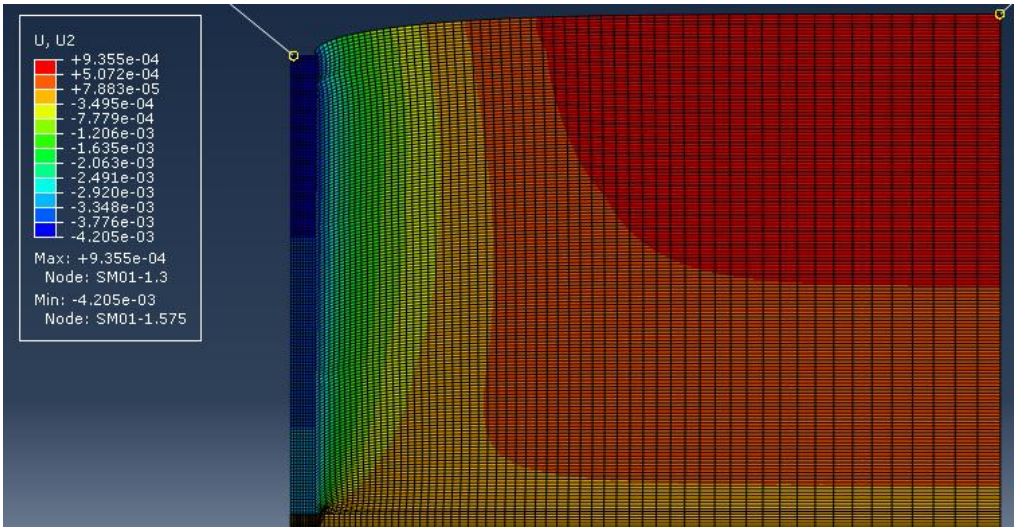

Figure 15. Vertical displacement (m) for SM-01 model

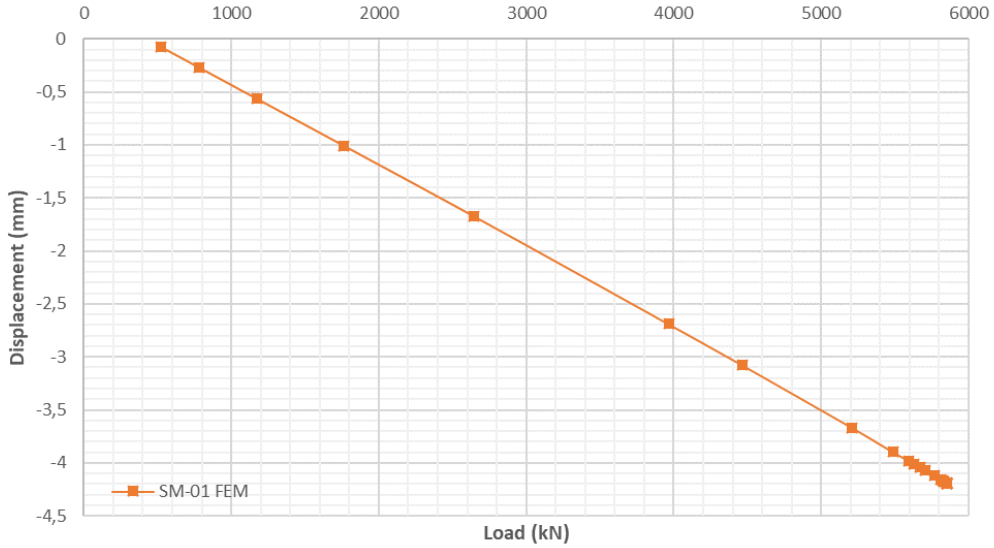

Figure 16. Load versus displacement elaborated through FEM for SM-01

3.4 Modeling results for SM-02

The parameters for modeling SM-02 profile are presented in Table 3. Results obtained for this region are directly represented in terms of load versus displacement in Fig. 17.

The maximum load value obtained, 14,101.8 kN, is nearly three times SM-01 maximum load. The displacement for this load value is 3.58 mm. This result could be associated with the fact that the pile toe penetrates 20 cm the altered rock layer.

Table 3. Soil parameters for SM-02 model

Soil	Average N_{SPT}	E (MPa)	ν	Specific weight (kN/m³)	ϕ (°)	C (Pa)
Const. Waste (sand)	-	10	0.2	16	34	$1.0x10^3$
Yellowish coarse sand	6	16.2	0.2	16	30.4	$1.0x10^3$
Yellowish silty sand	11	23.1	0.3	17	32.4	$1.0x10^3$
Orange sandy silt	30	67.5	0.4	18	40.0	$1.0x10^3$
Altered rock	-	$2.0x10^4$	0.2	20	-	-
Pinky granite	-	$4.7\ x10^4$	0.2	26	-	-
Concrete 45MPa	-	$3.40\ x10^4$	0.2	25	-	-

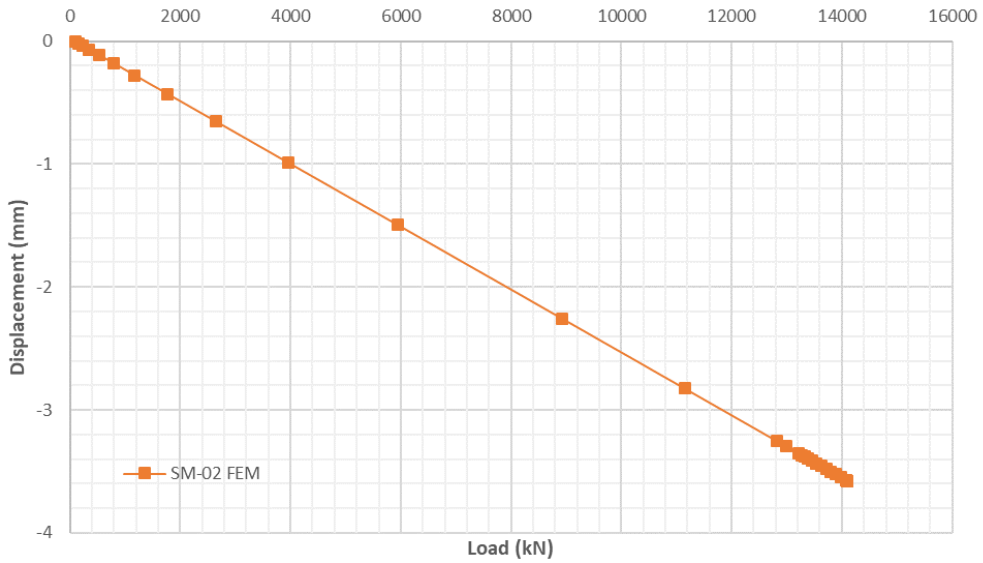

Figure 17. Load versus displacement elaborated through FEM for SM-02

3.5 Modeling results for SM-03

The parameters used to represent SM-03 sounding profile are presented in Table 4. From the load versus displacement curve, Fig. 18, it is observed that the bearing capacity corresponds to 5,201.5 kN with its displacement equal to 5.81 mm.

Table 4. Soil parameters for SM-03 model

Soil	Average N_{SPT}	E (MPa)	ν	Specific weight (kN/m³)	ϕ (°)	C (Pa)
Sand and const. waste	-	10	0.2	16	34	$1.0x10^3$
Brownish medium sand	7	18.9	0.2	16	30.8	$1.0x10^3$
Grayish coarse sand	17	45.9	0.3	17	34.8	$1.0x10^3$
Orange Sandy silt	31	69.75	0.4	18	40.4	$1.0x10^3$
Altered rock	-	$2.0x10^4$	0.2	20	-	-
Pinky granite	-	$4.7\ x10^4$	0.2	26	-	-
Concrete 45MPa	-	$3.40\ x10^4$	0.2	25	-	-

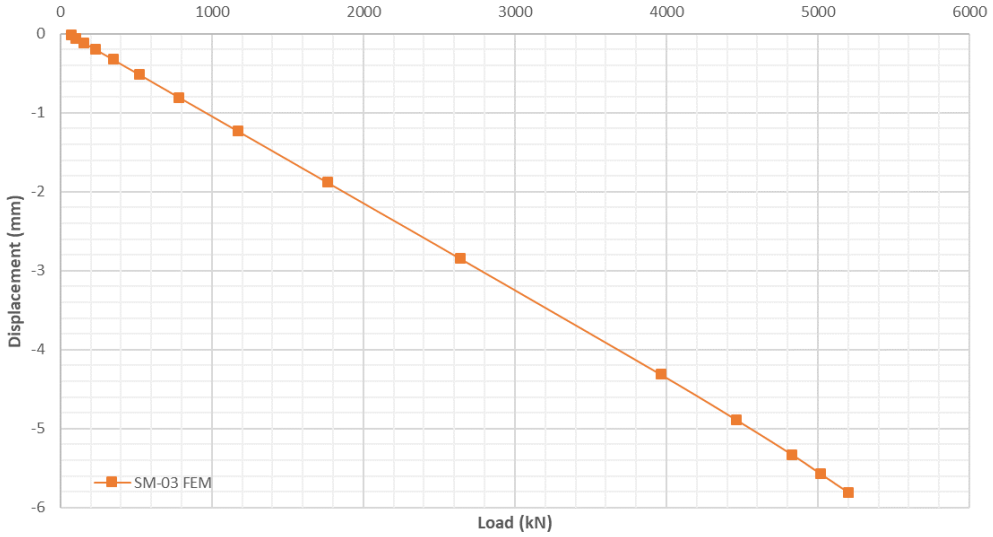

Figure 18. Load versus displacement elaborated through FEM for SM-03

3.6 Modeling results for SM-04

The parameters used in the modeling for SM-04 region are presented in Table 5 and the load versus displacement obtained is presented in Fig. 19. The load versus displacement curve indicates a bearing capacity of 6,100.2 kN with a displacement of 4,71 mm. This value approximates the results of SM-01 and 03.

Table 5. Soil parameters for SM-04 model

Soil	Average N_{SPT}	E (MPa)	ν	Specific weight (kN/m³)	ϕ (°)	C (Pa)
Sand and const. waste	-	10	0.2	16	34	$1.0x10^3$
Brownish medium sand	7	18.9	0.2	16	30.8	$1.0x10^3$
Grayish coarse sand	18	48.6	0.3	17	35.2	$1.0x10^3$
Orange medium sand	13	35.1	0.3	17	33.2	$1.0x10^3$
Orange sandy silt	34	76.5	0.4	18	41.6	$1.0x10^3$
Altered rock	-	$2.0x10^4$	0.2	20	-	-
Pinky granite	-	$4.7 x10^4$	0.2	26	-	-
Concrete 45MPa	-	$3.40 x10^4$	0.2	25	-	-

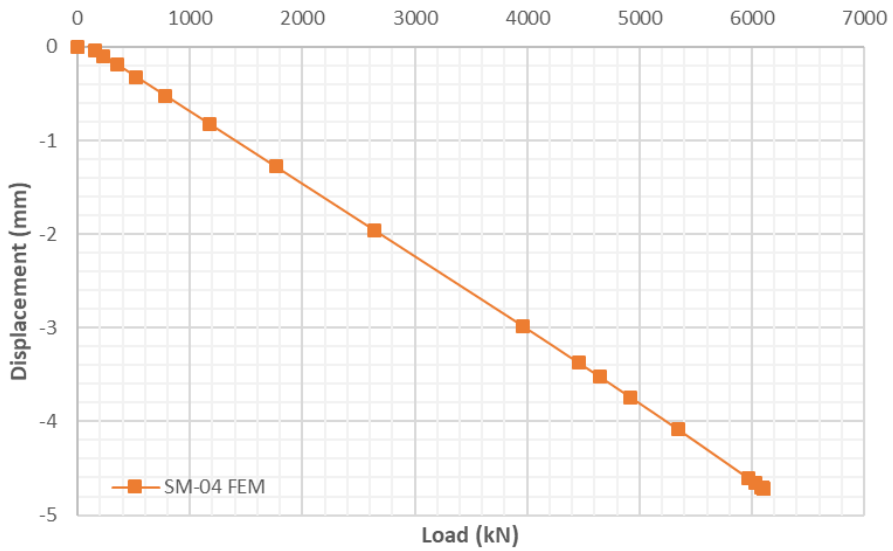

Figure 19. Load versus displacement elaborated through FEM for SM-04

3.7 Model sensitivity analysis

The parameters adopted for modeling are of great importance in determining the results. Since these parameters have been established from empirical equations, it is expected that the results do not faithfully represent the soil behavior. For the analysis of the parameters used, it was decided to vary the values of modulus of elasticity and friction angle of SM-01 model. The soil profile SM-01 is the closest to the pile where the bidirectional static load test was performed.

First, the elasticity modulus (E) of the three layers where N_{SPT} values were determined (grayish coarse sand, yellowish silty sand, and orange sandy silt) was varied. E values were varied to plus and minus 10 MPa. Parameters of the other layers, altered rock, pinky granite and concrete were kept constant in the analysis. The result is shown in Fig. 20. Subsequently, for the same reference layers (grayish coarse sand, yellowish silty sand, and orange sandy silt) the friction angle was increased to plus and minus 10°. Result is shown in Fig. 21.

It is concluded from the analysis of the figures that the variation in the modulus of elasticity (E) directly influences the slope of the curve, tending to approach what was determined in the load test when increasing the modulus. The variation of the friction angle causes the change in the limit resistance, leading the soil to higher loads until failure verification.

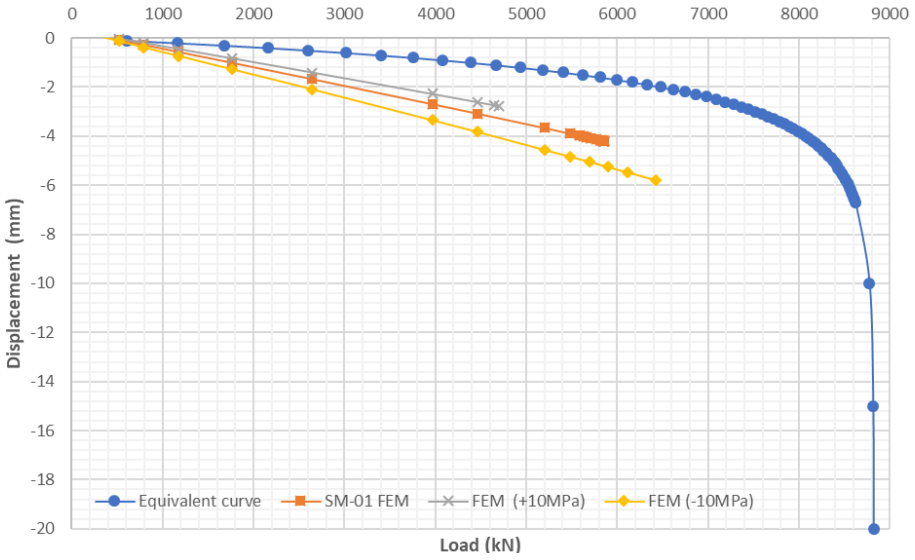

Figure 20. Variation of E modulus and comparison with equivalent curve

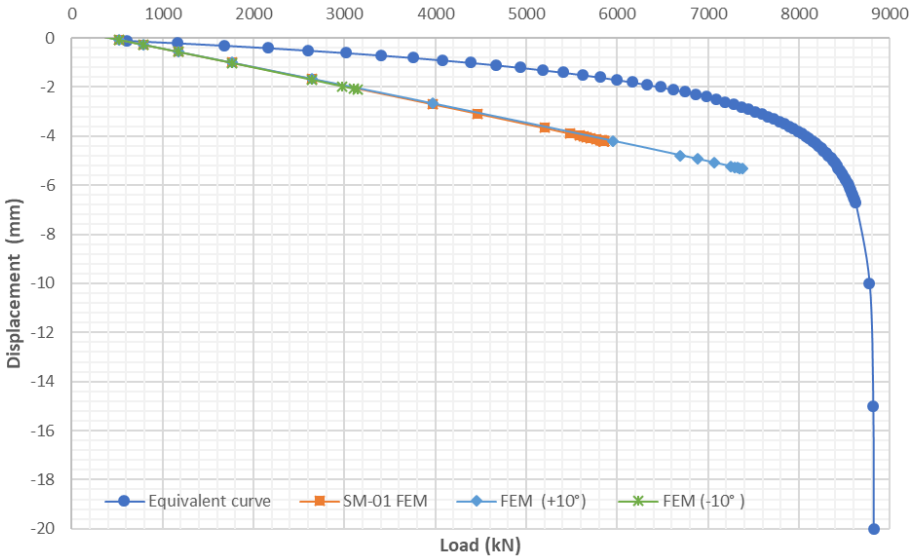

Figure 21. Variation of friction angle and comparison with equivalent curve

3.8 Comparative analysis among FEM and Bidirectional static load and Semiempirical methods

In this section results of the FEM method, bidirectional static load and semiempirical methods are directly compared. The semiempirical methods are Aoki and Velloso (AK), Décourt and Quaresma (DQ), Lobo (UFRGS), Teixeira (TX) and Bustamante and Gianeselli (BG). Results of the semiempirical methods were computed following the classical assumptions of each related author. More information for this subject can be found at classical literature (Cintra and Aoki [10], Velloso and Lopes [11], Hachich et al [12], Bustamante and Gianeselli [13]), and for the Hercílio Luz Bridge in Andrade [14].

Fig. 22 for region SM-01 shows the values obtained for each method and their relation to the value obtained by the bidirectional static load test (PCE-03). It is noted that all semiempirical methods present higher values than the load test. On the other hand, FEM provides lower bearing capacity, about 33.6% below the load test.

For SM-02 region Fig. 23 is presented. Comparison with the load test result demonstrates that all methods have bearing capacity significantly higher than those determined in PCE-03.

Concerning SM-03 region, Fig. 24 indicates that again the resistance obtained by FEM is lower than PCE-03 value. From this, it is possible to conclude that FEM usually provides lower resistances, which could indicate conservative parameters.

Result for SM-04 region is shown in Fig. 25. The method that most closely approximates what was observed in the field is the UFRGS method, which is above that observed in the field by 5.5%. The Bustamante-Gianeselli method, furthest from PCE-03 resistance value, is 202.1% higher. FEM model is the closest to the load test value. However, the value obtained is lower than 30.8%.

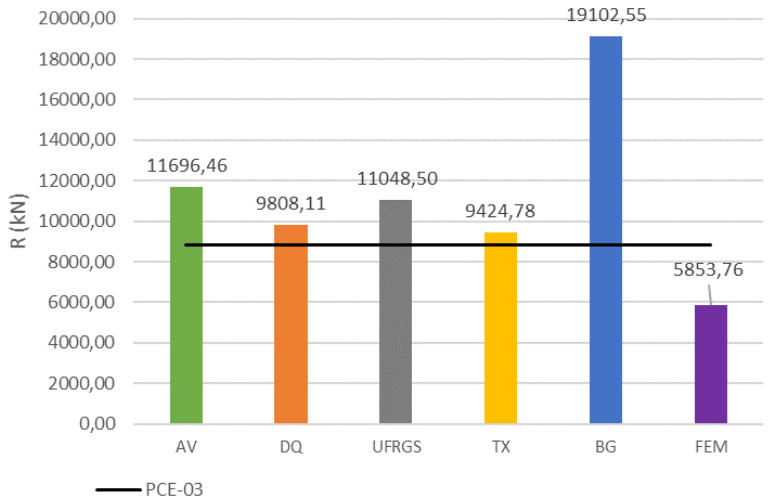

Figure 22. Comparison for SM-01

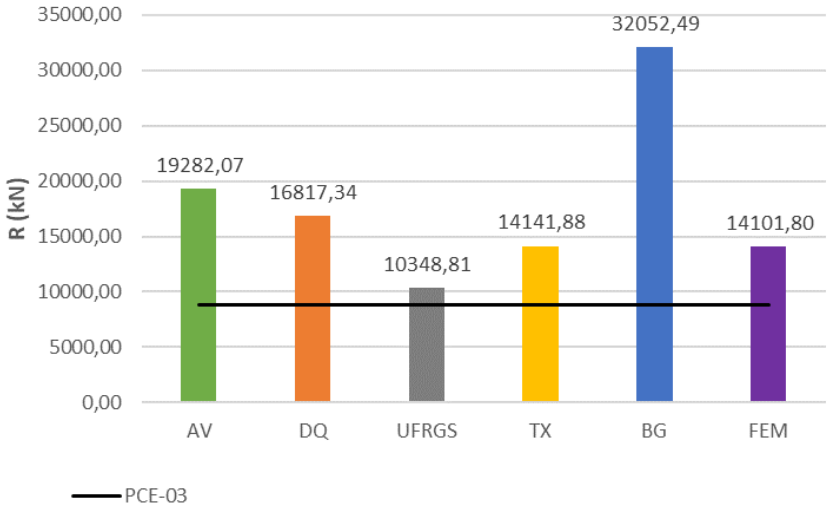

Figure 23. Comparison for SM-02

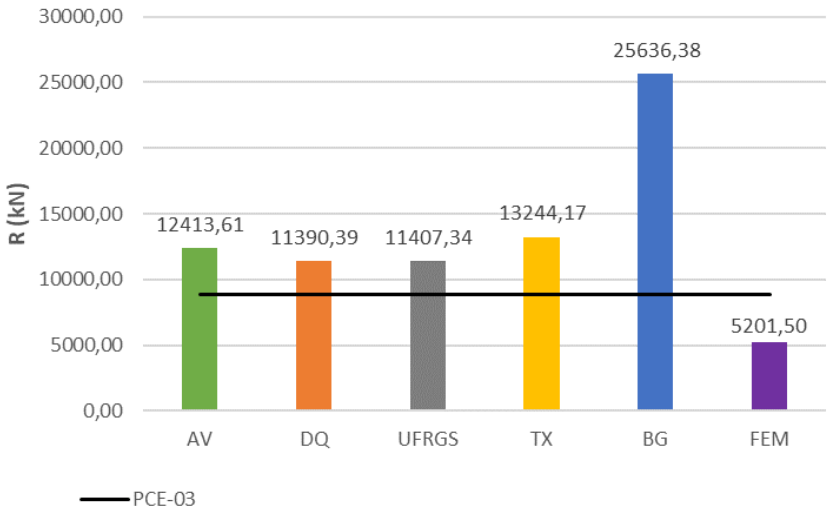

Figure 24. Comparison for SM-03

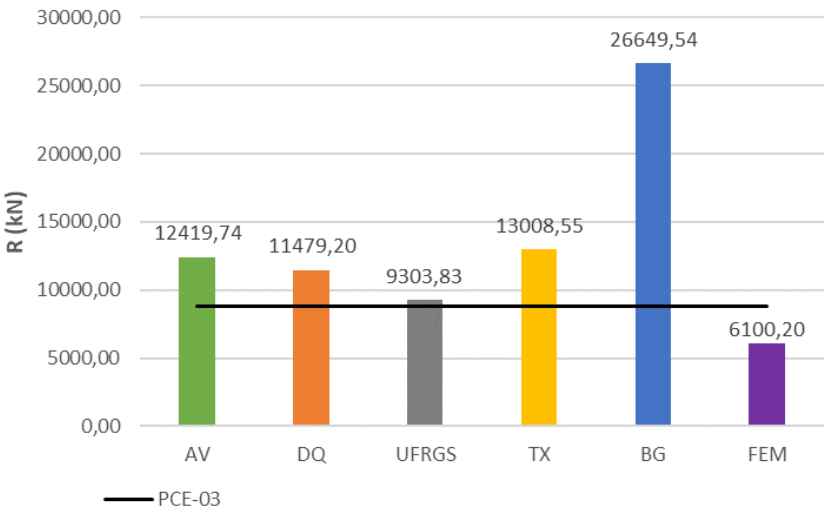

Figure 25. Comparison for SM-04

4 Conclusions

Using FEM software is a practice commonly used to study more complex problems. In the present paper, a model of a pile and soil layers has been created and studied. The difficulty in constructing a representative model consisted mainly in determining the soil resistance parameters. These parameters were determined based on average N_{SPT} values for each layer, implying a rough characterization of the problem.

Results obtained from the models for each soil profile allowed the evaluation of shear stress, normal stress, and displacements. With the data of normal stress and displacements, it was possible to draw load versus displacement curves.

The comparison between the different methods showed that the ultimate resistances determined by the FEM were usually below the load test value. This fact is directly associated with the uncertainty of the adopted parameters, determined through empirical equations. The semiempirical methods for all soil profiles resulted in higher resistances than the one determined by the bidirectional static load test.

The ultimate resistance determined by the load test when compared to the maximum workload, corresponding to 3,550.4 kN, indicates that there is a large resistance reserve and the safety of the massif is guaranteed.

This study reinforces the importance of the use of safety factors because uncertainties are normal for both soil characteristics and methods. It was observed the variation between methods and among soil profiles, even with a small distance between them.

Acknowledgements

Special thanks to the Federal University of Santa Catarina (UFSC) for making this paper possible.

We would also like to extend our gratitude to the Santa Catarina State Department of Infrastructure (DEINFRA) and Teixeira Duarte Ltda. for helping to get the data that supported this paper**.**

References

[1] Teixeira Duarte Ltda. Technical report: Continental side anchorage massif (PHL.TD.005.NT011) (in Portuguese). Florianópolis, 2017.
[2] Brazilian Association of Technical Standards. NBR 6118: Design of concrete structures – Procedure. Rio de Janeiro, 2014.
[3] Teixeira Duarte Ltda. Technical report: Continental Anchorage massif foundation: integrity tests and static load test (PHL.TD.005.NT016) (in Portuguese). Florianópolis, 2018.
[4] Brazilian Association of Technical Standards. NBR 6122: Design and construction of foundations. Rio de Janeiro, 2010.
[5] P.E.C.A.F. Silva. Hydrodynamic Expansive Cell: A new way to carry load tests (in Portuguese). In: 8º Congresso Brasileiro de Mecânica dos Solos e Engenharia de Fundações, COBRAMSEF, Porto Alegre, Brazil, v. 6, p. 223-241, 1986.
[6] C. van der Veen (1953). The bearing capacity of a pile. International Conference on Soil Mechanics and Foudation Engineering, 3., v.2.
[7] F. Falconi and V. L. Maset. Practical Analysis of Bidirectional test results (in Portuguese). In: 8° COBRAMSEG, Belo Horizonte. 2016.
[8] J. C. A. Cintra; N. Aoki; J. H. Albiero. Shallow foundation: geotechnical design (in Portuguese). São Paulo: Oficina de Textos. 2011.
[9] L. G. de Vallejo et al. Geological Engineering (in Spanish). Madrid: Pearson Educación. 2002.
[10] J. C. A. Cintra; N. Aoki. Pile foundation: geotechnical design (in Portuguese). São Paulo: Oficina de Textos. 2010.
[11] D. A. Velloso; F. R. Lopes. Foundations, vol. 2: Deep foundations (in Portuguese). São Paulo: Oficina de Textos. 2010.
[12] W. Hachich et al. Foundations: Theory and practice (in Portuguese). São Paulo: Pini. 1998.
[13] M. Bustamante; L. Gianeselli. Pile bearing capacity prediction by means of static penetrometer CPT. In: Second European Symposium on Penetration Testing. Amsterdam, 1982.
[14] G. D. Andrade. Bearing capacity analysis of the Hercílio Luz bridge anchorage massif foundations (in Portuguese). Federal University of Santa Catarina (UFSC). 2019.